Ecological Complexity 61 (2025) 101115

Contents lists available at ScienceDirect

Ecological Complexity

journal homepage: www.elsevier.com/locate/ecocom

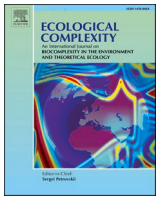

Ecological and environmental factors influencing exclusion patterns of phytoplankton size classes in lake systems

Sze-Wing To [a,b,*], Esteban Acevedo-Trejos [c], Sherwood Lan Smith [d,e], Subhendu Chakraborty [b], Agostino Merico [b,a]

[a] School of Science, Constructor University, Bremen, Germany
[b] Systems Ecology Group, Leibniz Centre for Tropical Marine Research (ZMT), Bremen, Germany
[c] Earth Surface Process Modelling, German Research Centre for Geoscience (GFZ), Potsdam, Germany
[d] Advanced Institute for Marine Ecosystem Change (WPI- AIMEC), JAMSTEC, Yokohama, Japan
[e] Earth SURFACE Research Centre, Research Institute for Global Change (JAMSTEC), Yokohama, Japan

ARTICLE INFO

Keywords:
Phytoplankton coexistence
Richness
Competitive exclusion
Ecological trade-off
Grazing strategy
Allometric relationships
Size-based model

ABSTRACT

For decades, ecologists have been intrigued by the paradoxical coexistence of a wide range of phytoplankton types on a seemingly limited number of resources. The interactions between environmental conditions and trade-offs emerging from eco-physiological traits of phytoplankton are typically proposed to explain coexistence. The number of coexisting types over ecological time scales reflects what we call here 'exclusion patterns', that is, the temporal removal of certain phytoplankton types due to competition. Despite many observational and mathematical modelling efforts over the last two decades, we still know surprisingly little, in quantitative terms, about how the interplay of nutrient regimes and specific zooplankton grazing strategies affects the exclusion patterns of competing phytoplankton types. Phytoplankton types can be distinguished according to many different traits. Among various morphological traits, phytoplankton cell size is considered one of the most meaningful in explaining crucial eco-physiological processes, including nutrient uptake and zooplankton grazing. Here we use a size-based plankton model to investigate exclusion patterns of phytoplankton size classes over ecological time scales and under varying environmental conditions. We performed numerical experiments under different allometric scaling relationships, different combinations of specialist and generalist grazing strategies, different inorganic nutrient regimes, and different mixing frequencies. We quantified exclusion patterns by using two metrics: (1) coexistence, defined here as the average number of size classes present over the first 30 days of the simulations, and (2) exclusion time scale, defined here as the time required to outcompete 80 % of the size classes present in the system at the beginning of the simulations. Under low nutrient regimes, we found that the impact of grazing on the exclusion patterns of phytoplankton was almost negligible. Under high nutrient regimes, different exclusion patterns emerged depending on the grazing strategy. When the community of zooplankton was dominated by generalist grazers, we found higher coexistence and longer exclusion time scales of phytoplankton size classes than when the community of zooplankton was dominated by specialist grazers. We further found that the combined effects of grazing strategies and allometric relationships on the size structure of the phytoplankton community were significant and non-trivial. We thus argue that plankton models disregarding these processes may miss relevant drivers of phytoplankton community assembly and trait diversity.

1. Introduction

The coexistence of different phytoplankton species over ecological time scales reflects patterns of community structure (HilleRisLambers et al., 2012). Phytoplankton richness (reflecting the number of coexisting species) was understood to be constrained by bottom-up processes, particularly by the competition for resources (Tilman 1982; Grover 1990). The theory suggested that inferior competitors for a limiting resource should decline over time and should eventually be outcompeted (Hardin, 1960). However, ecologists also observed that the

* Corresponding author at: School of Science, Constructor University, Campus Ring 1, 28759, Bremen, Germany.
E-mail addresses: sto@constructor.university (S.-W. To), esteban.acevedo-trejos@gfz-potsdam.de (E. Acevedo-Trejos), lanimal@jamstec.go.jp (S.L. Smith), subhendu.chakraborty@leibniz-zmt.de (S. Chakraborty), agostino.merico@leibniz-zmt.de (A. Merico).

https://doi.org/10.1016/j.ecocom.2024.101115
Received 18 December 2023; Received in revised form 23 October 2024; Accepted 31 October 2024
Available online 30 December 2024

number of coexisting phytoplankton species consistently exceeds the number of limiting resources, a phenomena known as the plankton paradox (Hutchinson, 1961). Multiple mechanisms have been put forward to explain this evident paradox, including resource partitioning, temporal and spatial heterogeneities, and predatory interactions (Chesson, 2000; Roy and Chattopadhyay, 2007). What is often overlooked in the study of plankton communities is the crucial role that herbivores play in structuring phytoplankton communities and coexistence. Coexistence is promoted by apparent competition (Holt, 1977), whereby more competitive species experience stronger grazing pressure (Chesson, 2018). The maintenance of diversity depends, nevertheless, on the mediation of bottom-up and top-down interactions (Gaedke and Ebenhöh, 1991; Chase et al., 2002).

Seasonally changing abiotic factors or nutrient concentrations can regulate phytoplankton coexistence. The interplay between environmental variations and community dynamics has been studied for phytoplankton from a trait perspective, especially in relation to cell size (Gaedke, 1993; Litchman et al., 2007; Edwards et al., 2013). Given that organisms cannot invest an equal amount of energy in all traits, various trade-offs emerge between traits. As environmental conditions change, organisms with the fittest set of traits under the given conditions will be inevitably favored. Trait-based and size-based modelling studies found that trade-offs are primary drivers of phytoplankton community structure and diversity (reviewed in Follows and Dutkiewicz, 2011; Acevedo-Trejos et al., 2022). Those models explored the mediating effects of trade-offs between, for example, light and nutrient acquisition abilities (Bruggeman and Kooijman, 2007), and nutrient affinity and grazing avoidance ability (Acevedo-Trejos et al., 2018). A modelling study based on a chemostat system found that the trade-off between phytoplankton growth and inorganic nutrient acquisition can promote phytoplankton coexistence by delaying competitive exclusion under nutrient enriched conditions (Göthlich and Oschlies, 2015). However, competitive exclusion time scales and the effects of size-based trade-offs on the coexistence of multiple phytoplankton sizes have received little attention.

The trade-off between phytoplankton nutrient uptake abilities and susceptibility of being grazed has important ecological consequences for phytoplankton coexistence. The global ocean modelling studies of Prowe et al. (2012) and Vallina et al. (2014) suggested that prey-switching (simulated through the so-called kill-the-winner approach) is essential for promoting phytoplankton coexistence. Size-based models that considered a trade-off between nutrient uptake abilities and grazing susceptibilities were capable of producing size variation and diversity patterns of phytoplankton consistent with marine observations (Banas, 2011; Ward et al., 2012; Acevedo-Trejos et al., 2018; Taherzadeh et al., 2019). In these modelling studies, higher nutrient uptake abilities by small phytoplankton cells were offset by a higher susceptibility of being grazed by zooplankton. However, observations and laboratory experiments (Saiz and Calbet, 2007; Chen and Liu, 2010; Edwards et al., 2012; Marañón et al., 2013; Hillebrand et al., 2022) showed that these empirically-derived allometric relationships can be fraught with uncertainties, particularly in relation to the maximum growth rate of phytoplankton and the maximum ingestion (or clearance) rate of zooplankton. The consequences of these uncertainties for the predictions of ecosystem models have yet to be assessed.

Zooplankton grazing exerts a strong control on phytoplankton diversity. Grazing strategies arising from zooplankton prey selectivity strongly impact the community structure of phytoplankton through the emergence of grazing refugia (Lürling, 2021). Zooplankton can select on phytoplankton abundance or particular traits. In this respect, zooplankton can be categorized as generalists or specialists, with generalists being less selective than specialists. The ecosystem model of Prowe et al. (2012) showed that, by selecting more abundant prey, zooplankton grazing creates refugia for phytoplankton that are weak competitors for inorganic nutrients, thereby facilitating the coexistence of phytoplankton with different traits. The ecosystem model of Chenillat et al. (2021) suggested that the shape of grazing refugia affects the diversity of phytoplankton functional groups. Another planktonic model showed that an absolute selectivity based solely on prey functions also led to a general decline in biodiversity (Ryabov et al., 2015). A plankton model comprised of one zooplankton grazer and two competing phytoplankton showed that the generalist grazer led to lower phytoplankton coexistence than the specialist grazer (Cropp et al., 2017). While these studies investigated the effects of zooplankton grazing strategies on phytoplankton dynamics, it is not well-understood how different combinations of grazing strategies can interact with other environmental factors (e.g., nutrient availability) to modulate the coexistence of different phytoplankton size classes.

Here we present a size-based model to determine how phytoplankton nutrient uptake and zooplankton grazing influence exclusion patterns of phytoplankton communities in lake ecosystems. We conducted numerical experiments under different allometric scaling relationships, different combinations of size-selective grazing strategies (specifically, specialist and generalist), and different nutrient regimes and mixing frequencies. We quantified the resulting exclusion patterns with two metrics: (1) coexistence, which we defined as the average number of size classes present over the first 30 days of the simulations and (2) exclusion time scale, which we defined as the time it takes to temporarily exclude (or outcompete) 80 % of the size classes present in the system at the beginning of the simulations. Our study aims to elucidate how different nutrient levels and grazing strategies interact with an ecological trade-off, based on data-driven allometric relationships, to influence the coexistence of phytoplankton size classes in lake ecosystems.

2. Materials and methods

2.1. Size-based model description

We created a size-based plankton model to simulate the coexistence of different phytoplankton types under varying environmental conditions (Fig. 1). The trophic interactions in the model were quantified by the energy flows via various ecological processes (Fig. 1). The model comprises multiple phytoplankton size classes (P_i, with $i = 1, 2, \ldots, 150$) whose growth is limited by light and nutrients. The phytoplankton community is subject to size-selective grazing by zooplankton of different body sizes (Z_j, with $j = 1, 2$) and with different grazing strategies, specialist and generalist. Generalists feed on a wider range of prey sizes than specialists. We considered nitrogen (N) as the model single currency so that all state variables are expressed in terms of μmol N L^{-1}.

By adopting the classic slab physics approximation (Fasham et al., 1990; Post et al., 2024), the modelled lake is subdivided into an upper well-mixed layer and a bottom nutrient-rich layer, with the boundary between them being defined by the variable depth of the upper mixed layer (henceforth the Mixed Layer Depth, MLD; Fig. 1). In most lake ecosystems, the exchange of biomass fluxes between the two layers is driven by physical processes. In our model, physical processes include (1) diffusive mixing between the upper layer and the bottom layer on non-motile (nutrient, detritus, and phytoplankton) entities and (2) differential effects on motile (zooplankton) and non-motile entities due to changes in MLD. These processes are captured by the following term (Evans and Parslow, 1985):

$$\lambda = \frac{\omega + h^{+}(t)}{MLD(t)}, \tag{1}$$

where ω is the cross-thermocline mixing constant, representing diffusive mixing. $h^{+}(t)$ quantifies changes of biomass fluxes corresponding to variations in MLD and is given by,

$$h^{+}(t) = \max(0, h), \tag{2}$$

with $h = \frac{dMLD(t)}{dt}$. When the MLD shallows ($h < 0$), a portion of the non-

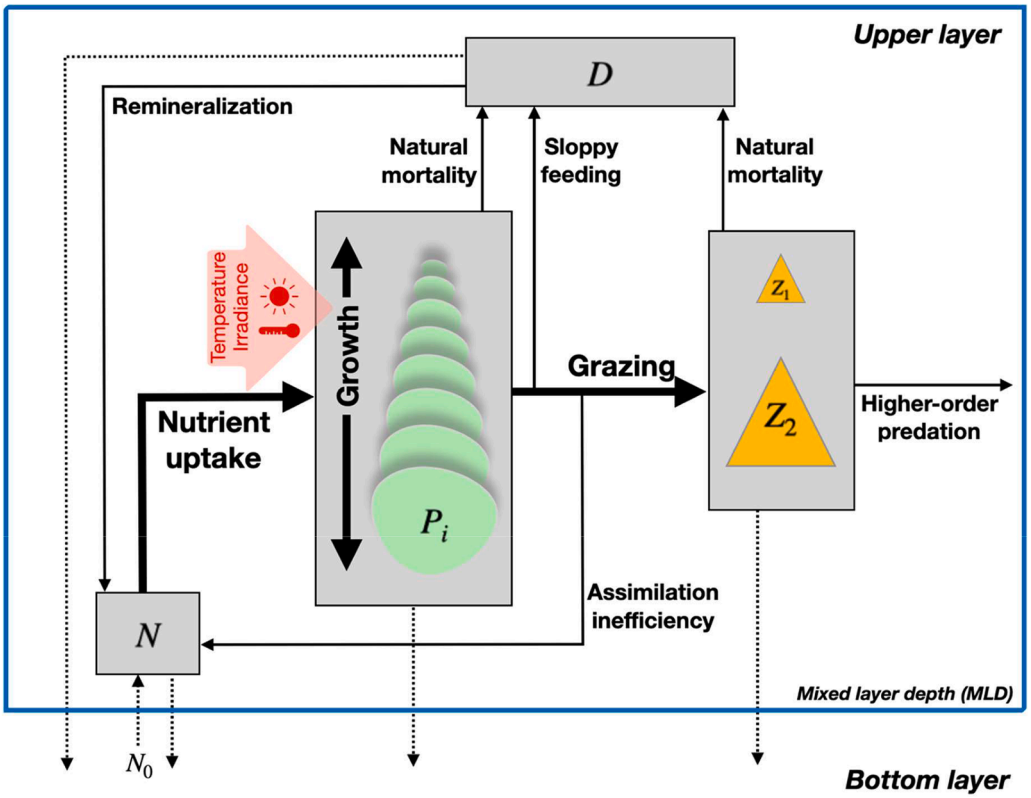

Fig. 1. Components and processes of the size-based plankton model. The model adopts a 0D spatial configuration by adopting a simple two-layer slab physics. The upper layer (assumed to be homogeneously mixed) contains the plankton ecosystem consisting of four components, inorganic nutrient, N, phytoplankton, P, zooplankton, Z, and detritus, D. Phytoplankton are subdivided into 150 size classes (P_i, with $i = 1, 2, \ldots, 150$) and zooplankton are subdivided into 2 size classes, Z_1 and Z_2. Thick black arrows represent size-dependent processes for phytoplankton nutrient uptake, phytoplankton growth, and zooplankton grazing. Thin black arrows represent biogeochemical (solid lines), ecological (solid lines), and mixing (dotted lines) processes, which are size-independent. The large red arrow indicates the environmental variables (temperature and irradiance) that, in addition to inorganic nutrients, limit phytoplankton growth. The environmental variables are input data used as model forcing. The loss of zooplankton to higher-order predators is density-dependent and represented by a quadratic function. We assumed that the loss of nutrients from the upper layer is replenished through mixing events by a constant nutrient source, N_0, in the bottom layer.

motile entities (i.e., nutrient, phytoplankton, and detritus) are detrained from the shallowing upper layer but the associated decreasing volume of water is assumed to leave the concentrations of these entities unchanged (hence $h^+(t) = 0$). When MLD deepens ($h > 0$), these three entities are diluted (hence producing a positive value for the mixing term λ, which is a loss term). Zooplankton were considered motile and thus capable of maintaining themselves in the upper layer; a shallowing or a deepening of the MLD would, respectively, increase or decrease their concentrations. Thus, mixing term of zooplankton is:

$$\lambda_z = \frac{h}{MLD(t)}. \tag{3}$$

A key feature of the model is the characterization of planktonic communities in terms of eco-physiological trait relationships and grazing strategies. We considered a total of four allometric relationships, as follows:

$$\mu_{max_i}\left(S_i^P\right) = \beta_{\mu_{max}} S_i^{P\ \alpha_{\mu_{max}}}, \tag{4}$$

$$K_{N_i}\left(S_i^P\right) = \beta_{K_N} S_i^{P\ \alpha_{K_n}}, \tag{5}$$

$$I_{max_j}\left(S_j^Z\right) = \beta_{I_{max}} S_j^{Z\ \alpha_{Imax}}, \tag{6}$$

$$P_{opt_j}\left(S_j^Z\right) = \beta_{P_{opt}} S_j^{Z\ \alpha_{Popt}}. \tag{7}$$

These relationships describe: the maximum growth rate (Eq. (4)) and the half-saturation constant for nutrient uptake (Eq. (5)) of each phytoplankton size class, i; and the maximum ingestion rate (Eq. (6)) and the optimal prey size (Eq. (7)) of each zooplankton size class, j. S_i^p and S_j^Z indicate, cell size and body size of, respectively, phytoplankton and zooplankton (in μm). The parameters α and β are, respectively, exponent and intercept of the allometric functions (Eq. (4)-(7)).

We focused on the effects that zooplankton specialists and generalists have on the coexistence of phytoplankton size classes in a milieu of interactions determined by bottom-up (nutrient uptake by phytoplankton) and top-down (grazing by zooplankton) processes. Next, we present the formulations of different model components and describe the numerical experiments.

2.1.1. Phytoplankton and zooplankton

The temporal dynamics of biomass P_i for the i^{th} phytoplankton size class is determined by:

$$\frac{dP_i}{dt} = (\mu_i - - \phi_P - - \lambda)P_i - \sum_i \sum_j G_{ij} Z_j, \tag{8}$$

with

$$\mu_i = \mu_{max_i}\left(S_i^P\right) \frac{N}{K_{N_i}\left(S_i^P\right) + N} E(T) H(I_z) \tag{9}$$

Phytoplankton growth, μ_i (Eq. (9)) is controlled by (1) a size-dependent maximum growth rate term, $\mu_{max_i}\left(S_i^P\right)$ (Eq. (4)), (2) a size- and nutrient-dependent nutrient uptake term, following Monod (1949), $\left(\frac{N}{K_{N_i}\left(S_i^P\right) + N}\right)$, (3) a temperature-regulated growth term,

$$E(T) = e^{0.063T}, \tag{10}$$

with T indicating Lake Surface Temperature (LST) in °C, and (4) a light-limited growth term,

$$H(I_z) = \frac{1}{MLD}\int_{Z=0}^{Z=MLD} P_I(z)dz \tag{11}$$

The light limitation growth term depends on the daily MLD-averaged photosynthesis rate and is obtained by integrating the photosynthesis-irradiance relationship, $P_I(z)$, following Lewis and Smith (1983) through depth z. $P_I(z)$ is given by,

$$P_I(z) = P_{max}\frac{\alpha_{P_I}\cdot I(z)}{\sqrt{P_{max}^2 + [\alpha_{P_I} I(z)]^2}}, \tag{12}$$

where P_{max} denotes maximum photosynthetic rate, α_{P_I} indicates the initial slope for $P_I(z)$, and $I(z)$ is the irradiance I calculated at depth z based on the Beer-Lambert's law,

$$I_z = I_0 \cdot e^{-K_{par}\cdot z}. \tag{13}$$

In Eq. (13), I_0 is the irradiance at lake surface (i.e. at depth $z = 0$) and K_{par} represents a total light attenuation coefficient due to water. For Eq. (11) (the integral of the light limitation growth term), we considered the analytical solution proposed by Anderson et al. (2015):

$$H(I_z) = \frac{1}{MLD}\int_{z=0}^{z=MLD} P_I(z)dz = \frac{P_{max}}{K_{par}MLD}\log\left(\frac{\alpha_{P_I}I_0 + \sqrt{P_{max}^2 + (\alpha_{P_I}I_0)^2}}{\alpha_{P_I}I(z) + \sqrt{P_{max}^2 + [\alpha_{P_I}I(z)]^2}}\right) \tag{14}$$

The losses of phytoplankton biomass are determined by mixing, λ (Eq. (1)), natural mortality, ϕ_P, and zooplankton grazing, $\sum_i\sum_j G_{ij}Z_j$.

The temporal dynamics of biomass Z_j for the j^{th} zooplankton size class is described by the following equation:

$$\frac{dZ_j}{dt} = \left(\varepsilon\gamma\sum_i\sum_j G_{ij}Z_j - _Z - \eta_Z Z_j - \lambda_z\right)Z_j \tag{15}$$

with

$$G_{ij} = I_{max_j}\left(S_j^Z\right)\frac{\delta_{ij}\left(S_i^P,\ S_j^Z\right)P_i}{K_p + \sum_i\delta_{ij}\left(S_i^P,\ S_j^Z\right)P_i} \tag{16}$$

and

$$\delta_{ij}\left(S_i^P,\ S_j^Z\right) = e^{-\left(\frac{\log_{10}\left(S_i^P\right) - \log_{10}\left[P_{opt_j}\left(S_j^Z\right)\right]}{\theta_j}\right)^2}. \tag{17}$$

The first term in Eq. (15) describes the net gain from grazing, which reflects the fraction of ingested phytoplankton (ε) and the fraction of assimilated phytoplankton (γ). The assimilation of phytoplankton is assumed to occur instantaneously. The portion that is not ingested, $(1-\varepsilon)\sum_i\sum_j G_{ij}Z_j$), resulting, for example, from sloppy feeding, is immediately lost into the detritus pool. The fraction of phytoplankton that is not assimilated, $\varepsilon(1-\gamma)\sum_i\sum_j G_{ij}Z_j$), is immediately excreted into the nutrient pool. The value of ε and γ are assumed to be size-independent (Hansen et al., 1997). Following Banas (2011), the grazing rate G_{ij} (Eq. (16)) is determined by (1) the size-dependent maximum ingestion rate $I_{max_j}\left(S_j^Z\right)$ (Eq. (6)), (2) the half-saturation constant for phytoplankton, K_p, and (3) the grazing preference, $\delta_{ij}\left(S_i^P,\ S_j^Z\right)$ (Eq. (17)). The grazing preference is described by a unimodal function between 0 and 1 over the phytoplankton size spectrum. The median of the function is described by $P_{opt_j}\left(S_j^Z\right)$ and reflects the optimal prey size (Eq. (7)). Zooplankton losses (Eq. (15)) includes natural mortality (ϕ_Z), higher order predation ($\eta_Z Z_j$), and mixing, λ_z (Eq. (3)).

2.1.2. Nutrient and detritus

The temporal dynamics of nutrient (N) and detritus (D) are given by:

$$\frac{dN}{dt} = -\sum_i\mu_i P_i + \varphi D + \varepsilon\ (1 - _ - \gamma)\sum_i\sum_j G_{ij}Z_j + \lambda(N_0 - _ - N). \tag{18}$$

$$\frac{dD}{dt} = \sum_i\phi_P P_i + \sum_j\phi_z Z_j + (1 - _ - \varepsilon)\sum_i\sum_j G_{ij}Z_j - (\varphi + \lambda)D. \tag{19}$$

The first term in Eq. (18) describes the nutrient outflow from phytoplankton uptake. The nutrient pool is fueled by the remineralization of detritus, φD, and by the fraction of phytoplankton that is not assimilated during grazing, $\varepsilon\ (1 - _ - \gamma)\sum_i\sum_j G_{ij}Z_j$. The last term in Eq. (18), $\lambda(N_0 - _ - N)$, describes the nutrient exchange between upper and bottom layers through mixing where N_0 represents a constant source of nutrient in the bottom layer. The detritus pool collects organic materials from mortalities and the unconsumed portion of phytoplankton by zooplankton (sloppy feeding). All variables in this model are subject to a mixing loss rate, λ (Table 1).

2.2. Numerical experiments

We experimented systematically with a range of conditions, including different (1) scenarios of grazing strategies, (2) resource availabilities, based on inorganic nutrient inputs and mixing frequencies, and (3) allometric scaling relationships for μ_{max} and I_{max} (Table 2). We considered a phytoplankton community of 150 size classes evenly spaced on a $\log_{10}$ basis, from 1 to 100 μm in Equivalent Spherical Diameter (hereafter ESD). We considered two herbivorous zooplankton differing in body size, a nano-grazer of 5 μm (Z_1) and a micro-grazer of 200 μm (Z_2). All variables were initialized with the same low concentrations, 0.01 μmol N L^{-1}.

The forcing variables in our model were: Mixed Layer Depth (MLD), Lake Surface Temperature (LST), and Photosynthetically Active Radiation (PAR). For LST and PAR, we used averaged weather data for lakes around 40° N relative to the period 1991 – 2011 (Supp. Fig. S1A) from Layden et al. (2015). Reflecting the average lake depth of eight Swiss lakes (Pomati et al., 2020), the seasonal variation of the MLD in the model varied from 2.5 to 80 m. The MLD followed a sinusoidal function with frequencies varying over a one-year period (Supplementary Material S1, Fig. S1B). The varying frequencies of the MLD allowed us to perform numerical experiments under different mixing regimes.

We adopted a set of standard allometric relationships derived from a rich compilation of over 120 freshwater phytoplankton species and 28 zooplankton species (Hansen et al., 1994, 1997; Edwards et al., 2012), illustrated in Fig. 2A-D. These allometric relationships produce an eco-physiological trade-off, in which small phytoplankton cells possess better nutrient uptake and growth abilities than large phytoplankton cells but are exposed, in turn, to higher zooplankton grazing pressures.

2.2.1. Grazing scenarios

We investigated the effects of zooplankton grazing strategies by examining a series of grazing scenarios. Two grazing strategies, specialist and generalist, were determined by the size tolerance θ_j of 0.2 and 0.5, respectively. The grazing rates resulting from the allometric relationships for I_{max} (Eq. (6)) configured Z_1 and Z_2 as the dominant nano-grazer and the subordinate micro-grazer, respectively. The dominant grazer was determined by the highest maximum ingestion rate, I_{max} (Fig. 2B). The grazing target was additionally constrained by the

Table 1
List of parameters considered in the model with corresponding symbols, description, default values, units, and sources.

Symbol	Description	Value	Unit	Source
P_{max}	Maximum photosynthesis rate	1.1	d^{-1}	this study
α_{P_I}	Initial slope of P-I curve	0.15	Ein m^{-2} D^{-1}	this study
K_{par}	Light attenuation coefficient	0.1	m^{-1}	Fasham et al. (1990)
ω	Cross-thermocline mixing coefficient	0.1	m day^{-1}	Fasham et al. (1990)
N_0	Scenarios of nutrient supplied from the bottom water layer	1, 15, 50	μmol N L^{-1}	this study
ϕ_P	Natural mortality – phytoplankton	0.2	d^{-1}	this study
ϕ_Z	Natural mortality – zooplankton	0.1	d^{-1}	this study
η_Z	Higher-order mortality rate – zooplankton	0.34	d^{-1}	Oschlies & Schartau (2005)
ε	Ingestion efficiency (e.g., due to sloppy feeding)	0.69	–	Fasham et al. (1990)
γ	Assimilation efficiency	0.75	–	Oschlies & Schartau (2005)
φ	Remineralization rate	0.6	d^{-1}	this study
K_p	Half-saturation constant – zooplankton	3	μmol N L^{-1}	this study
θ_j	Prey size tolerance	0.2 (specialist) 0.5 (generalist)	μm	Banas (2011), Hansen et al. (1994)
S_i^P	Cell sizes – phytoplankton	1–100	μm	this study
S_j^Z	Body sizes – zooplankton	5 (Z_1) 200 (Z_2)	μm	this study
$\beta_{\mu_{max}}$	Intercept of allometric relationship for μ_{max_i}	$10^{-.69}$	d^{-1}	Edwards et al. (2012)
$\alpha_{\mu_{max}}$	Exponent of allometric relationship for μ_{max_i}	−0.36	–	Edwards et al. (2012)
β_{K_N}	Intercept of allometric relationship for K_{N_i}	$10^{-0.71}$	μmol N L^{-1}	Edwards et al. (2012)
α_{K_N}	Exponent of allometric relationship for K_{Ni}	0.52	–	Edwards et al. (2012)
$\beta_{I_{max}}$	Intercept of allometric relationship for I_{maxj}	26	d^{-1}	Hansen et al. (1997)
$\alpha_{I_{max}}$	Exponent of allometric relationship for I_{maxj}	−0.4	–	Hansen et al. (1997)
$\beta_{P_{opt}}$	Intercept of allometric relationship for P_{opt_j}	0.65	μm	Hansen et al. (1994)
$\alpha_{P_{opt}}$	Exponent of allometric relationship for P_{opt_j}	0.56	–	Hansen et al. (1994)
N_0, P_0, Z_0, D_0	Initial conditions for all state variables	0.01	μmol N L^{-1}	this study

allometric relationship for P_{opt} (Eq. (7)), such that the dominant small grazer fed voraciously on small phytoplankton and the subordinate large grazer fed mildly on intermediate size classes of phytoplankton (Fig. 2D). We examined all possible combinations of grazing strategies, resulting in four scenarios (Table 2): dominant specialist with subordinate specialist (SS, Fig. 2E), dominant specialist with subordinate generalist (SG, Fig. 2F), dominant generalist with subordinate specialist (GS, Fig. 2G), and dominant generalist with subordinate generalist (GG, Fig. 2H). These four grazing scenarios were further combined with different inorganic nutrient regimes and mixing frequencies.

Table 2
Parameter values considered in the numerical experiments. The experiments were created by changing the values of the parameters defining 1) grazing strategies, 2) environmental conditions (nutrient levels and mixing frequencies), and 3) allometric scaling relationships for μ_{max} and I_{max}. For every grazing scenario, we performed simulations under three nutrient levels, and, for every nutrient level, we performed simulations under three mixing frequencies (for a total of 36 simulations). Experiments with different allometric relationships were performed at a fixed nutrient regime (eutrophic) and for every grazing scenario we performed simulations under the three mixing frequencies (for a total of 12 simulations). All experiments were based on the standard parameter values presented in Table 1, unless otherwise specified.

Grazing scenarios	Nutrient levels	Mixing frequencies	Allometric scalings	
			$\alpha_{\mu_{max}}$	$\alpha_{I_{max}}$
SS: dominant specialist with subordinate specialist	Oligotrophic: 1 μmol N L^{-1}	Constant: no mixing events	−0.36 (standard)	−0.4 (standard)
SG: dominant specialist with subordinate generalist	Eutrophic: 15 μmol N L^{-1}	Medium: 4 mixing events $year^{-1}$	−0.54	−0.4
GS: dominant generalist with subordinate specialist	Hypertrophic: 50 μmol N L^{-1}	High: 12 mixing events $year^{-1}$	−0.18	−0.4
GG: dominant generalist with subordinate generalist	Eutrophic: 15 μmol N L^{-1}		−0.36	−0.6
			−0.36	−0.2

2.2.2. Nutrient regimes and mixing frequencies

We examined how coexistence and exclusion of phytoplankton varied under different nutrient levels. The nutrient levels were co-determined by nutrients supplied from the bottom layer (N_0) and by mixing frequencies. For nutrient, we considered oligotrophic, eutrophic, and hypertrophic conditions corresponding, respectively, to 1, 15, and 50 μmol N L^{-1} (Table 2). For mixing frequencies, we considered constant, medium, and high mixing corresponding, respectively, to no mixing, 4 mixing events per year, and 12 mixing events per year (Table 2, Supp. Fig. S1B). We considered nitrate, NO_3^-, as the single nutrient source for phytoplankton growth.

2.2.3. Variations in allometric scaling

We considered variations in the allometric relationship for the maximum growth rate of phytoplankton, μ_{max}, and for the maximum ingestion rate of zooplankton, I_{max}. We changed the parameter values of $\alpha_{\mu_{max}}$ and $\alpha_{I_{max}}$ by ±50 % from their respective standard values of −0.36 and −0.4 (Table 2). Higher values of $\alpha_{\mu_{max}}$ and $\alpha_{I_{max}}$ led to flatter allometric relationships, whereas lower values led to steeper relationships (Fig. 2A-B). A higher $\alpha_{\mu_{max}}$ enhanced the growth ability of phytoplankton but reduced differences in growth abilities between size classes (Fig. 2A). Likewise, a higher $\alpha_{I_{max}}$ increased the grazing pressure on phytoplankton and the increment was proportionally higher for large cells (Fig. 2B). These variations revealed the effects of flatter or steeper allometric relationships on the coexistence of phytoplankton size classes.

2.2.4. Quantification of phytoplankton exclusion patterns

Exclusion pattens were defined as the different coexistence trajectories of phytoplankton size classes emerging from environmental variation over ecological timescales. However, we did not address permanent extinction or evolutionary processes. A size class was excluded from the system once its abundance fell below 0.01 μmol N L^{-1}, which was the starting abundance assigned to all size classes. We analysed our results in relation to two quantities: (1) the average number of size classes present over the first 30 days of the simulations, which we called, “coexistence”, and (2) the time it took to exclude (or outcompete) 80 %

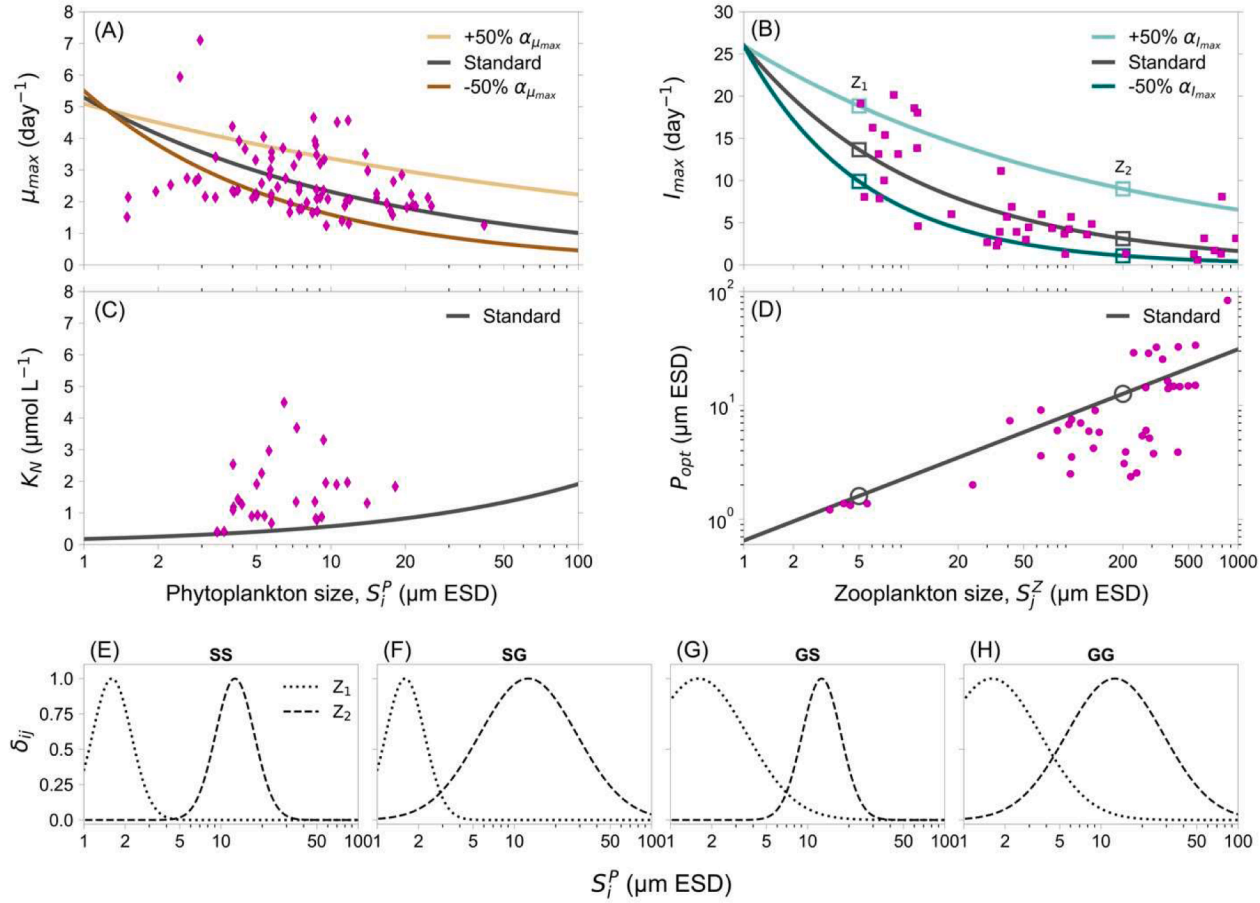

Fig. 2. Data-driven allometric relationships and grazing strategies considered in this study. Allometric relationships determining (A) maximum growth rates for phytoplankton, μ_{max} and (C) half-saturation constant for nutrient, K_N, with phytoplankton size S_i^P. Allometric relationships determining (B) maximum ingestion rates for zooplankton, I_{max} and (D) optimal prey size, P_{opt}, with zooplankton size S_j^Z. Dark solid lines represent a standard set of allometric scaling derived from data compilations of Edwards et al. (2012), Hansen et al. (1994), and Hansen et al. (1997) represented, respectively, with diamonds, dots, and squares. Open symbols indicate values considered for the zooplankton grazers, Z_1 and Z_2. The lines in (A) and (B) are the allometric relationships considered in this study, the standard $\alpha_{\mu_{max}}$ and $\alpha_{I_{max}}$, and the ±50 % variations from the standards. Grazing scenarios (E-H) for different combinations of specialist and generalist represented, respectively, by narrow and wide kernels drawn in relation to grazing preferences, δ_{ij}. The S_i^P at the maximum δ_{ij} corresponds to the P_{opt} shown in panel D.

of the size classes present at the beginning of the simulations ($n = 150$), which we called "exclusion time scale" (Fig. 3). The exclusion time scale also provided a relative metric for assessing changes in size diversity.

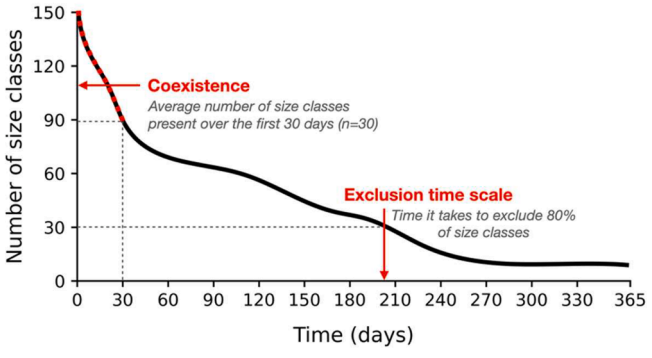

Fig. 3. Conceptual description of the two metrics considered to quantify exclusion patterns. We defined "coexistence" the average number of size classes present over the first 30 days of the simulations. We defined "exclusion time scale" the time it takes to exclude (or outcompete) 80 % of the size classes present at the beginning of the simulations ($n = 150$). A size class was considered excluded from the system once its abundance fell below 0.01 µmol N L^{-1}.

3. Results

3.1. Different nutrient regimes and mixing frequencies

The change in the number of size classes over time depended on nutrient regimes. Under oligotrophic conditions, we observed the steepest negative slopes, indicating the strongest declines in the number of phytoplankton size classes in the first 5 days of the simulations. After these initial sharp declines, the number of size classes stabilized to very low levels (Fig. 4). Under eutrophic and hypertrophic conditions, the rates of decline were generally lower than under oligotrophic conditions (Fig. 4). The highest rates of exclusion were observed under oligotrophic conditions, with only one size class left at day 365 (Supp. Fig. 2, panel A, C, E, and G). This single remaining size class was the smallest (1 µm) in the system (Supp. Fig. 2, panel B, D, F, and H). This extreme level of exclusion produced the lowest coexistence (<20 size classes at median level, Fig. 5A) and the shortest exclusion time scale (<5 days at median level, Fig. 5B). Increasing mixing frequency resulted in lower coexistence but this effect was weak and disappeared with time for most grazing scenarios (Supp. Fig. S3 insets and S4). As the nutrient regime changed from oligotrophic to eutrophic and hypertrophic, pronounced oscillations were observed in the number of size classes. These oscillations were driven by oscillatory dynamics in predator-prey abundances, depending on the specific grazing strategy (see Fig. S5).

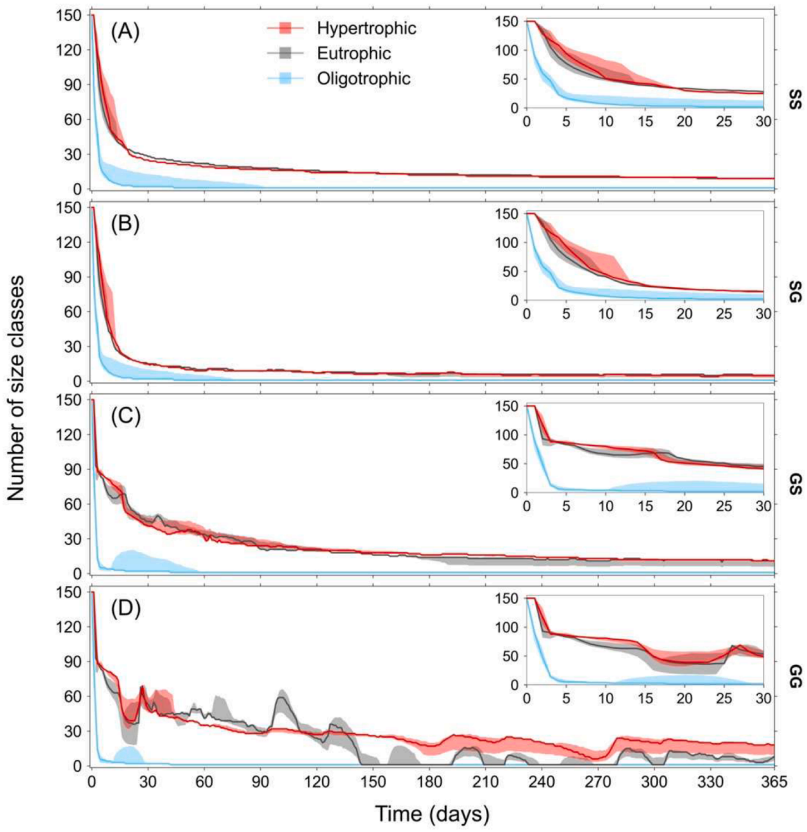

Fig. 4. Number of phytoplankton size classes over 365 days obtained under varying environmental conditions (nutrient regimes and mixing frequencies) and for different grazing scenarios. The colours indicate different nutrient regimes: light-blue for oligotrophic (1 μmol N L^{-1}); grey for eutrophic (15 μmol N L^{-1}); and red for hypertrophic (50 μmol N L^{-1}). For every grazing strategy, we performed simulations under the three nutrient regimes, and for every nutrient regime, we performed simulations under the three mixing frequencies. For every nutrient regime, the continuous lines and the shaded areas represent, respectively, the median (50th percentile) and the interquartile range (i.e. the 25th and 75th percentiles) of the results obtained with the three mixing frequencies (constant, medium, and high). The insets magnify the first 30 days. These results were generated with standard allometric relationships.

3.2. Different grazing scenarios

Under oligotrophic conditions, the number of size classes were similar in the different grazing scenarios (Fig. 4) and the biomass of the grazer was relatively low (Supp. Fig. S5). Under eutrophic and hypertrophic conditions, the change in the number of size classes over time depended on grazing scenarios. Specifically, the coexistence and the exclusion time scale depended on the grazing strategy of the dominant grazer ("SS" and "SG" versus "GS" and "GG"). When the dominant strategy was specialist, "SS" and "SG", the declining trend in the number of size classes was steady after 10 days (Fig. 4A-B, insets), 6 days longer than when the dominant strategy was generalist, "GS" and "GG" (Fig. 4C-D, insets). The grazing scenarios characterized by a dominant generalist showed pronounced fluctuations in phytoplankton size classes, especially under eutrophic conditions (Fig. 4D, grey curve). These fluctuations reflected high-frequency variations in phytoplankton mean size along the decline in size classes (Supp. Fig. S6). The fluctuations in size classes persisted even until the 10th year (Supp. Fig. S7). We observed a higher coexistence in the scenarios dominated by a generalist (GS and GG), up to 70 size classes, than in the scenarios dominated by a specialist (SS and SG), up to 55 size classes (Fig. 5A). We also observed a longer exclusion time scale for GS and GG, between 60 and 120 days, than for SS and SG, between 10 and 30 days (Fig. 5B).

3.3. Variations of the allometric relationships under eutrophic and hypertrophic conditions

The variations in the allometric relationships, for the phytoplankton maximum growth rate (μ_{max}) and for the zooplankton maximum ingestion rate (I_{max}), were controlled by the parameters that describe the slope of the relationships, $\alpha_{\mu_{max}}$ and $\alpha_{I_{max}}$. These variations altered, respectively, the growth abilities of different phytoplankton and the grazing pressure on different phytoplankton (Fig. 2). Despite ±50 % variation in $\alpha_{\mu_{max}}$ and $\alpha_{I_{max}}$, the number of phytoplankton size classes decreased consistently over time (Fig. 6). In general, scenarios with the same dominant grazing strategy ("SS" and "SG" versus "GS" and "GG") responded similarly to changes in allometric scaling. The declines in size classes were faster when a specialist grazer dominated the system, "SS" and "SG" (Fig. 6A-D). Systems dominated by a generalist grazer, "GS" and "GG", were sensitive to changes in allometric relationships, as shown by the higher variability in the results (Fig. 6E-H). The number of phytoplankton size classes was more sensitive to allometries controlling for top-down ($\alpha_{I_{max}}$) rather than bottom-up ($\alpha_{\mu_{max}}$) pressure.

The variation in allometric relationships mediated the effects of the grazing strategy on the exclusion patterns of phytoplankton. In all grazing scenarios, higher $\alpha_{\mu_{max}}$ or lower $\alpha_{I_{max}}$ enhanced the coexistence and prolonged the exclusion time scale, whereas lower $\alpha_{\mu_{max}}$ or higher $\alpha_{I_{max}}$ reduced the coexistence and shortened the exclusion time (Fig. 7). However, the sensitivity of coexistence and exclusion time scale to variations in $\alpha_{\mu_{max}}$ or in $\alpha_{I_{max}}$ differed by grazing scenarios. For example, scenario "GG", produced a large difference between high and low $\alpha_{\mu_{max}}$ (Fig. 7). The standard condition of this scenario showed the highest coexistence (about 70 size classes) and the slowest exclusion time scale (up to 120 days). With a −50 % $\alpha_{\mu_{max}}$ or a + 50 % $\alpha_{I_{max}}$, this scenario showed reduced coexistence (30 to 40 size classes) and fast exclusion time scale (about 20 days) to levels similar to other grazing scenarios

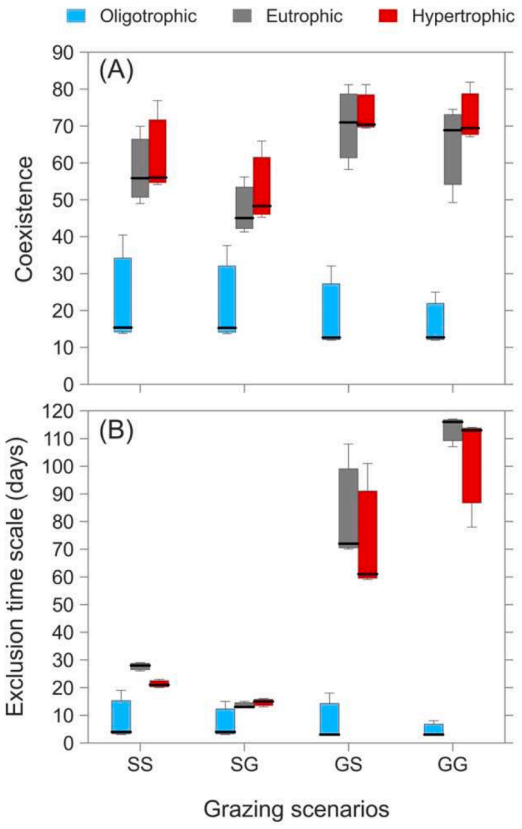

Fig. 5. Metrics for assessing exclusion patterns for different grazing strategies and nutrient regimes (colours). (A) Coexistence was defined as the average number of size classes present over the first 30 days of the simulations. (B) Exclusion time scale was defined as the time it takes to exclude (or outcompete) 80 % of the size classes present at the beginning of the simulations. The black lines inside the box plots and the widths of the whiskers represent, respectively, the median (50 % percentile) and the interquartile range (25 % and 75 % percentiles) of the results obtained with the three mixing frequencies (constant, medium, and high).

(Fig. 7). This result indicated that the effects of different grazing strategies on coexistence and exclusion time scale of phytoplankton size classes depended on the specific allometric relationship considered for growth and grazing.

4. Discussion

We investigated exclusion patterns of phytoplankton size classes under different environmental conditions (nutrient regimes and mixing frequencies), different allometric scaling relationships, and different zooplankton grazing strategies. We found that, under oligotrophic conditions, coexistence and exclusion time scales were independent of grazing strategies. In contrast, under eutrophic and hypertrophic conditions, dissimilar exclusion patterns emerged at different grazing strategies. While grazing strategies dominated by generalists enhanced the coexistence and prolonged the exclusion time scale, the number of size classes was more sensitive to variations in allometric relationships.

4.1. Effects of nutrient regimes and grazing on coexistence of phytoplankton cell sizes

Under oligotrophic conditions, the rates of decline in the number of phytoplankton size classes were fast irrespective of grazing strategies. This depended on the fact that low inorganic nutrients led to low phytoplankton biomass and, consequently, to low zooplankton biomass. A low zooplankton biomass exerted, in turn, a weaker top-down control on phytoplankton. In this case, the number of coexisting phytoplankton size classes was mainly driven by competition for nutrient. Additionally, oligotrophic conditions allowed only the smallest size class (1 μm) to survive in the system because of their high affinity for nutrients. The dominance of small phytoplankton under oligotrophic conditions was in line with both the competitive exclusion principle (Hardin, 1960) and competition theory (Tilman, 1982). The competitive exclusion principle states that only the fittest size class survives under limited resources, while competition theory predicts the survival of the species with the greatest nutrient acquisition ability. Our study indicated that nutrient competition was the main factor driving low phytoplankton coexistence under oligotrophic conditions.

Under eutrophic and hypertrophic conditions, the impact of grazing became relevant to the coexistence of different phytoplankton size classes. Specifically, our results showed higher coexistence and longer exclusion time scales under eutrophic and hypertrophic conditions. In our model, higher nutrient concentrations increased zooplankton biomass and caused a stronger top-down control on phytoplankton. This stronger top-down control exerted, in turn, a higher grazing pressure on the small phytoplankton (those with higher nutrient uptake abilities). These conditions relaxed competition for nutrient among phytoplankton and led to what we define here a grazer-mediated coexistence. As a result, when nutrient levels increased, the drivers of exclusion patterns shifted from bottom-up to top-down. Thus, the resulting exclusion patterns depended on the interaction of nutrient competition through a shared resource and apparent competition through shared grazers (Leibold, 1996; Poulin and Franks, 2010; Chesson, 2018). Previous size-resolved models found that phytoplankton size diversity was driven by a trade-off between nutrient acquisition and susceptibility to size-selective grazing (Poulin and Frank, 2010; Acevedo-Trejos et al., 2015, 2018). We showed here that a grazer-mediated coexistence emerged only under eutrophic and hypertrophic conditions, under relatively higher zooplankton biomass.

A recent modelling study (Branco et al., 2020), based on an eco-evolutionary trade-off between nutrient competition and grazing susceptibility found similar trends. They showed that community composition under low nutrient conditions that was dominated by small phytoplankton shifted to nutritionally-poor large phytoplankton under high nutrient conditions. Our results are also consistent with laboratory experiments and field observations. For example, (Karakoç et al., 2020) showed that the presence of ciliates increased bacterial coexistence due to the emergence of two predation-resistant bacterial species in a microcosm experiment. Chemostat studies (Steiner, 2003; Burson et al., 2018) showed that small cells dominated the phytoplankton community under low nutrient regimes and in the absence of grazing. Finally, observations in a nutrient-rich estuary (Cloern, 2017) suggested that the presence of grazing increased the abundance of large phytoplankton.

4.2. Role of grazing strategies in the coexistence of phytoplankton cell sizes

In our model, the grazing strategy played an important role in shaping the grazer-mediated coexistence of different phytoplankton size classes. Our results showed higher coexistence and longer exclusion time scales when generalists dominated the community of grazers. Our simulations produced different grazing effects, which depended on the body size of zooplankton. Enclosure experiments have shown similar results. Steiner (2001), for example, showed that phytoplankton diversity can be affected by the grazing characteristics of zooplankton (the small *Ceriodaphia* vs. the large *Daphnia*) as *Ceriodaphia* grazed on small phytoplankton species whereas *Daphnia* consumed large species. Our results are also consistent with a recent size-based bi-trophic grazing model, which showed that a generalist grazing strategy, produced by many specialist grazers feeding on the whole phytoplankton size spectrum, can foster higher phytoplankton diversity (Taniguchi et al., 2023). Ryabov et al. (2015), who used a generic trait-based planktonic model,

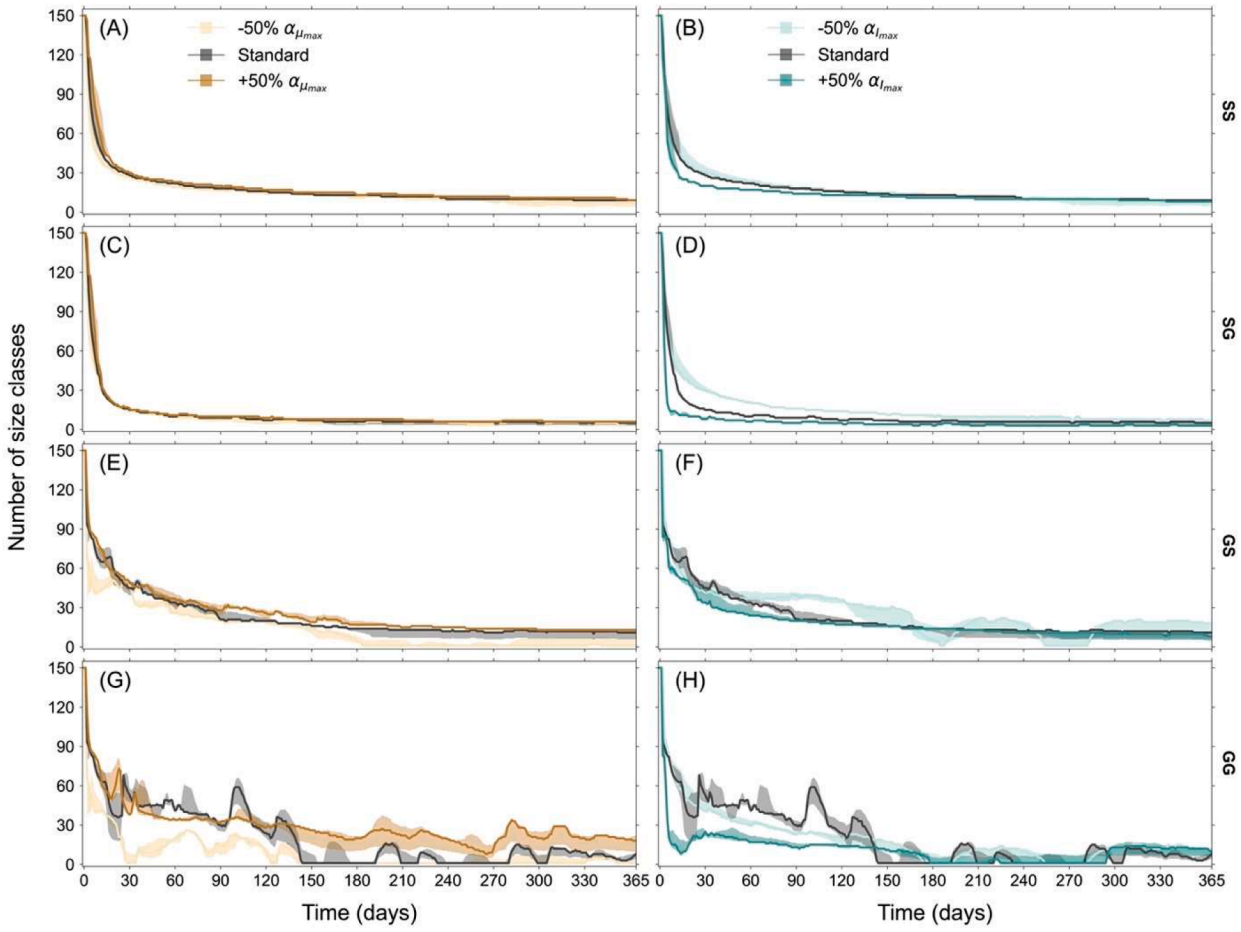

Fig. 6. Number of phytoplankton size classes resulting from varied allometric relationships (i.e., ±50 % variations in $\alpha_{\mu_{max}}$ and $\alpha_{I_{max}}$) and from different grazing scenarios. For every allometric relationship, we performed simulations under the three mixing frequencies (constant, medium, and high). The continuous lines and the shaded areas represent, respectively, the median (50 % percentiles) and the interquartile range (25 % and 75 % percentiles) of the results obtained with the three mixing frequencies. These results were generated under the eutrophic nutrient regime at 15 μmol N L^{-1}.

comprising a single-predator, obtained a similar result: a wide prey selectivity (equivalent to the generalist grazing strategy considered in our model) led to higher trait diversity in the prey community. When Ryabov et al. (2015) considered a narrow prey selectivity (equivalent to the specialist grazing strategy considered in our model), trait diversity declined, as in our case. Taken together, these studies suggest that the results we obtained on the grazing strategy are general and do not depend on the specific model structure considered.

When the zooplankton community was dominated by generalist grazers, we also found a high variation in phytoplankton mean size. Earlier studies found that herbivorous grazing enhances algal species diversity (Lubchenco, 1978; McCauley and Briand, 1979). Observations from nutrient-rich conditions, in laboratory experiments and lake mesocosms, showed that the presence of the generalist grazer *Daphnia* spp. (not larger than 250 μm) can promote species diversity of phytoplankton (Steiner, 2003; Sarnelle, 2005). How generalist grazing affects the size diversity (rather than the species diversity) of phytoplankton, however, remains unclear. Under eutrophic and hypertrophic conditions, our results showed a wider range of phytoplankton mean size when the generalist grazing is the dominant strategy. In our model, generalist grazers prevented the dominance of small phytoplankton and result in strong grazer-mediated coexistence. Therefore, we hypothesized that specialist grazers create grazing refugia in which small phytoplankton cells can escape grazing and can outcompete larger phytoplankton cells (e.g., Irigoien et al., 2005). Given the importance of phytoplankton size diversity on the functioning of aquatic ecosystems, our results highlighted the relevance of zooplankton size-selective grazing strategies. Plankton models disregarding these processes may thus miss relevant drivers of phytoplankton community assembly.

4.3. *Role of allometric relationships for phytoplankton growth and zooplankton grazing*

Variation in allometric scaling relationships for phytoplankton maximum growth rate (μ_{max}) and zooplankton maximum ingestion rate (I_{max}) can alter the grazer-mediated coexistence of generalist. Specifically, for systems dominated by generalist grazers, we found reductions in phytoplankton coexistence and shortenings of exclusion time scales when nutrient competition was severe (low $\alpha_{\mu_{max}}$) or when apparent competition was weak (high $\alpha_{I_{max}}$). Theoretical predictions upheld that selective grazing can promote or impede prey coexistence, depending on the trophic couplings between grazer and prey (Chase et al., 2002). Grounded on a size-based trophic coupling, our model results are in line with these theoretical predictions. First, we showed that specialist and generalist strategies produced different exclusion patterns. Second, our sensitivity analysis on the allometric relationships with eco-physiological properties revealed that the grazer-mediated coexistence is modulated by the interaction strengths between phytoplankton and zooplankton. Thus, our size-based model pointed to the modulating effects of size-selective grazing strategies and allometric relationships as the mechanisms shaping the coexistence of phytoplankton size classes over ecological time scales.

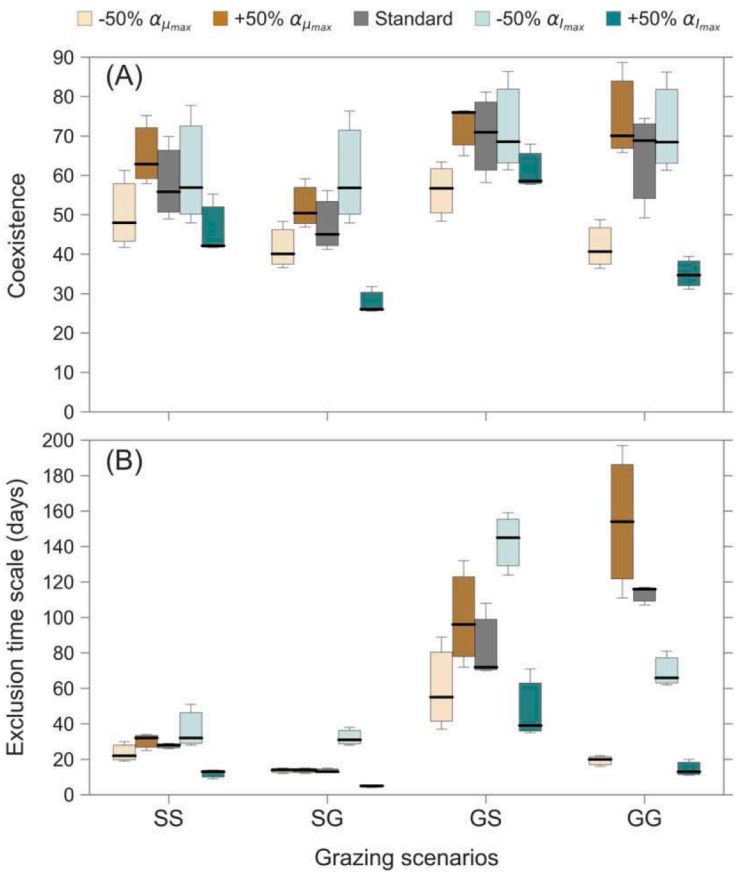

Fig. 7. Coexistence (A) and exclusion time scale (B) at varying (±50 %) allometric relationships and for different grazing scenarios. The black lines inside the box plots and the widths of the whiskers represent, respectively, the median (50 % percentile) and the interquartile range (25 % and 75 % percentiles) of the results obtained with the three mixing frequencies (constant, medium, and high). These results were generated under the eutrophic nutrient regime at 15 μmol N L^{-1}.

4.4. Limitations of our study and future research directions

Exclusion in our model is a deterministic process driven by nutrient availability and grazing in a closed system. In freshwater ecosystems, factors other than nutrient regimes and zooplankton grazing strategies could play a role in determining the coexistence of different phytoplankton types. The diversity of phytoplankton observed in lakes is often the outcome of diverse, interactive and seasonally-varying environmental factors. For example, the effects of temperature in our model are implemented in a simplified fashion via the monotonic, Eppley formulation (Eq. (10)), the same for all size classes. A potential limitation in our study is that we may miss physiological or ecological processes underpinning size-specific temperature responses. The effects of size-specific thermal tolerances on phytoplankton abundance and community structure under global warming scenarios are the object of our next study. Another caveat could be associated to the absence of allometric relationships in relation to light harvesting abilities. Previous light fluctuation experiments suggested that size-based competition for light can impact on phytoplankton species diversity (Litchman, 1998; Flöder et al., 2002). Analogously, chemostat competition experiments showed that phytoplankton shifted from competing for nutrient to competing for light as nutrient levels increased (Burson et al., 2018). Although conducted in the absence of grazing, these chemostat experiments suggested that resource co-limitations may have an impact on phytoplankton coexistence. The analysis of the effects produced by additional allometric relationships on phytoplankton coexistence goes beyond the scope of our study but constitutes interesting avenues for future research.

Our model is not spatially resolved and does not include dispersal processes, but spatial variation of environmental conditions and dispersal processes can affect the coexistence of different phytoplankton types. An idealized phytoplankton-zooplankton diffusion model (Behrenfeld et al., 2022) showed that competition for nutrient between phytoplankton cells of different sizes can be weakened when the phytoplankton community is spatially distributed, thus sustaining size diversity over a broad range of nutrient concentrations. Immigration of new types is an additional mechanism commonly able to sustain species diversity in simulated plankton communities (Acevedo-Trejos et al., 2016). Using data from a three-year study on a system of 34 interconnected, neighbouring ponds, Cottenie et al. (2001, 2003) found evidence of a metacommunity structure across the multiple ponds. Despite sharing the same water source, the ponds differed substantially in zooplankton community structure, indicating sustained diversity within the metacommunity. Building on the concept of metacommunities, Leibold and Norberg (2004) used theoretical arguments to suggest that the connectivity through dispersal of local communities embedded within metacommunities can enhance the diversity of such systems and thus their capacity to adapt to environmental change. The dispersal of zooplankton can also vary the grazer-mediated coexistence of phytoplankton cells by generating or eliminating grazer-free refugia (Limberger and Wickham, 2011). Note that also the ecological trade-off we considered can differ between local and regional scales when dispersal processes play an important role in influencing diversity patterns (Kneitel and Chase, 2004). Finally, a data analysis of phytoplankton metacommunities from >800 lake ecosystems in Finland emphasized the strong effect that spatial variations in nutrient concentrations may have in shaping phytoplankton diversity patterns (Weigel et al., 2023). Including all these many additional features in a model is neither a practical nor a desirable approach. As any other mathematical modelling endeavour, our study is grounded on a theoretical context and based on hypothetical "what if" scenarios. Thus, within the context

defined by our assumptions, our results highlight the synergistic effects that resource availability and grazing have on the diversity of lake phytoplankton. We argue that these aspects cannot be ignored by future modelling studies focused on real-world predictions.

5. Conclusions

In summary, we investigated the role of different nutrient regimes, grazing strategy, and allometric relationships, on the coexistence of phytoplankton size classes. We found that grazing does not play a relevant role under oligotrophic conditions. With low nutrient concentrations, the exclusion mechanisms were dominated by nutrient competition. In contrast, under eutrophic and hypertrophic conditions, the generalist grazing strategy supported higher coexistence and longer exclusion time scale for different phytoplankton cell sizes. Additionally, such support depended on the specific allometric relationships considered for growth and grazing, as these relationships affected trophic couplings between phytoplankton and zooplankton. Our study demonstrated how the grazer-mediated coexistence of phytoplankton communities depended on the interactions between grazing strategies and allometric relationships for growth and grazing. In theory, our results could be extended to other aquatic environments (e.g., marine environments). However, caveats could not be ignored regarding the physical assumption considered here (the slab physics, valid primarily for vertically mixed and closed systems) and the characteristics of nutrient availability and grazing pressure, which may be system-specific. For example, the different compositions of the zooplankton communities could generate contrasting top-down pressures in marine and freshwater systems, with relevant implications for the structure of phytoplankton communities (Sommer and Sommer, 2006). The size-based modelling framework introduced here, represent a flexible approach for studying interactive mechanisms in shaping community structures of phytoplankton and can be easily extended to include the impacts of additional factors like temperature.

Data availability statement

The dataset generated and analyzed for this study can be found in Zenodo (https://doi.org/10.5281/zenodo.5815387). The python code of the mathematical model used in this study is freely available on Github (https://github.com/systemsecologygroup/SbNPZD_Exclusion).

CRediT authorship contribution statement

Sze-Wing To: Writing – review & editing, Writing – original draft, Methodology, Formal analysis, Conceptualization. **Esteban Acevedo-Trejos:** Writing – review & editing, Writing – original draft, Supervision, Methodology, Conceptualization. **Sherwood Lan Smith:** Writing – review & editing, Conceptualization. **Subhendu Chakraborty:** Writing – review & editing, Supervision. **Agostino Merico:** Writing – review & editing, Writing – original draft, Supervision, Project administration, Methodology, Funding acquisition, Conceptualization.

Declaration of competing interest

The authors declare that they have no known competing financial interests or personal relationships that could have appeared to influence the work reported in this paper.

Acknowledgments

The contributions to this work were funded by the German Research Foundation (DFG) and Swiss National Science Foundation (SNF) as part of the project AQUASCOPE [Grant no. 412375259].

Supplementary materials

Supplementary material associated with this article can be found, in the online version, at doi:10.1016/j.ecocom.2024.101115.

Data availability

I have shared the link to my data/code at the Attach File step.

References

Acevedo-Trejos, E., Brandt, G., Bruggeman, J., Merico, A., 2015. Mechanisms shaping size structure and functional diversity of phytoplankton communities in the ocean. Sci. Rep. 5, 8918. https://doi.org/10.1038/srep08918.

Acevedo-Trejos, E., Brandt, G., Smith, S.L., Merico, A., 2016. PhytoSFDM version 1.0.0: phytoplankton size and functional diversity model. Geosci. Model Dev. 9, 4071–4085. https://doi.org/10.5194/gmd-9-4071-2016.

Acevedo-Trejos, E., Cadier, M., Chakraborty, S., Chen, B., Cheung, S.Y., Grigoratou, M., Guill, C., Hassenrück, C., Kerimoglu, O., Klauschies, T., Lindemann, C., Palacz, A., Ryabov, A., Scotti, M., Smith, S.L., Våge, S., Prowe, F., 2022. Modelling approaches for capturing plankton diversity (MODIV), their societal applications and data needs. Front. Mar. Sci. 9, 975414. https://doi.org/10.3389/fmars.2022.975414.

Acevedo-Trejos, E., Marañón, E., Merico, A., 2018. Phytoplankton size diversity and ecosystem function relationships across oceanic regions. Proc. R. Soc. B. 285, 20180621. https://doi.org/10.1098/rspb.2018.0621.

Anderson, T.R., Gentleman, W.C., Yool, A., 2015. EMPOWER-1.0: an efficient model of planktonic ecOsystems WrittEn in R. Geosci. Model Dev. 8, 2231–2262. https://doi.org/10.5194/gmd-8-2231-2015.

Banas, N.S., 2011. Adding complex trophic interactions to a size-spectral plankton model: emergent diversity patterns and limits on predictability. Ecol Modell 222, 2663–2675. https://doi.org/10.1016/j.ecolmodel.2011.05.018.

Behrenfeld, M.J., Bisson, K.M., Boss, E., Gaube, P., Karp-Boss, L., 2022. Phytoplankton community structuring in the absence of resource-based competitive exclusion. PLoS ONE 17, e0274183. https://doi.org/10.1371/journal.pone.0274183.

Branco, P., Egas, M., Hall, S.R., Huisman, J., 2020. Why do phytoplankton evolve large size in response to grazing? Am. Nat. 195, E20–E37. https://doi.org/10.1086/706251.

Bruggeman, J., Kooijman, S.A.L.M., 2007. A biodiversity-inspired approach to aquatic ecosystem modeling. Limnol. Oceanogr. 52, 1533–1544. https://doi.org/10.4319/lo.2007.52.4.1533.

Burson, A., Stomp, M., Greenwell, E., Grosse, J., Huisman, J., 2018. Competition for nutrients and light: testing advances in resource competition with a natural phytoplankton community. Ecology 99, 1108–1118. https://doi.org/10.1002/ecy.2187.

Chase, J.M., Abrams, P.A., Grover, J.P., Diehl, S., Chesson, P., Holt, R.D., Richards, S.A., Nisbet, R.M., Case, T.J., 2002. The interaction between predation and competition: a review and synthesis. Ecol Lett. 5, 302–315. https://doi.org/10.1046/j.1461-0248.2002.00315.x.

Chen, B., Liu, H., 2010. Relationships between phytoplankton growth and cell size in surface oceans: interactive effects of temperature, nutrients, and grazing. Limnol. Oceanogr. 55, 965–972. https://doi.org/10.4319/lo.2010.55.3.0965.

Chesson, P., 2018. Updates on mechanisms of maintenance of species diversity. J Ecol 106, 1773–1794. https://doi.org/10.1111/1365-2745.13035.

Chenillat, F., Rivière, P., Ohman, M.D., 2021. On the sensitivity of plankton ecosystem models to the formulation of zooplankton grazing. PLoS ONE 16, e0252033. https://doi.org/10.1371/journal.pone.0252033.

Chesson, P., 2000. Mechanisms of Maintenance of Species Diversity. Annu. Rev. Ecol. Syst. 31, 343–366. https://doi.org/10.1146/annurev.ecolsys.31.1.343.

Cloern, J.E., 2017. Why large cells dominate estuarine phytoplankton: large cells dominate in estuaries. Limnol. Oceanogr. 63, S392–S409. https://doi.org/10.1002/lno.10749.

Cottenie, K., Michels, E., Nuytten, N., De Meester, L., 2003. Zooplankton metacommunity structure: regional vs. local processes in highly interconnected ponds. Ecology 84, 991–1000. https://doi.org/10.1890/0012-9658(2003)084[0991:ZMSRVL]2.0.CO;2.

Cottenie, K., Nuytten, N., Michels, E., De Meester, L., 2001. Zooplankton community structure and environmental conditions in a set of interconnected ponds. Hydrobiologia 442, 339–350. https://doi.org/10.1023/A:1017505619088.

Cropp, R., Moroz, I., Norbury, J., 2017. The role of grazer predation strategies in the dynamics of consumer-resource based ecological models. J. Sea Res. 125, 34–46. https://doi.org/10.1016/j.seares.2017.05.003.

Edwards, K.F., Litchman, E., Klausmeier, C.A., 2013. Functional traits explain phytoplankton responses to environmental gradients across lakes of the United States. Ecology 94, 1626–1635. https://doi.org/10.1890/12-1459.1.

Edwards, K.F., Thomas, M.K., Klausmeier, C.A., Litchman, E., 2012. Allometric scaling and taxonomic variation in nutrient utilization traits and maximum growth rate of phytoplankton. Limnol. Oceanogr. 57, 554–566. https://doi.org/10.4319/lo.2012.57.2.0554.

Evans, G.T., Parslow, J.S., 1985. A model of annual plankton cycles. Biol. Oceanogr. 3, 327–347. https://doi.org/10.1080/01965581.1985.10749478.

Fasham, M.J.R., Ducklow, H.W., McKelvie, S.M., 1990. A nitrogen-based model of plankton dynamics in the oceanic mixed layer. J. Mar. Res. 48, 591–639. https://doi.org/10.1357/002224090784984678.

Flöder, S., Urabe, J., Kawabata, Z., 2002. The influence of fluctuating light intensities on species composition and diversity of natural phytoplankton communities. Oecologia 133, 395–401. https://doi.org/10.1007/s00442-002-1048-8.

Follows, M.J., Dutkiewicz, S., 2011. Modeling diverse communities of marine microbes. Annu. Rev. Mar. Sci. 3, 427–451. https://doi.org/10.1146/annurev-marine-120709-142848.
Gaedke, U., 1993. Ecosystem analysis based on biomass size distributions: a case study of a plankton community in a large lake. Limnol. Oceanogr. 38, 112–127. https://doi.org/10.4319/lo.1993.38.1.0112.
Gaedke, U., Ebenhöh, W., 1991. Predator-mediated coexistence of calanoid copepods in a spatially heterogeneous environment: a numerical simulation model. Ecol. Modell. 56, 267–289. https://doi.org/10.1016/0304-3800(91)90204-E.
Göthlich, L., Oschlies, A., 2015. Disturbance characteristics determine the timescale of competitive exclusion in a phytoplankton model. Ecol. Modell. 296, 126–135. https://doi.org/10.1016/j.ecolmodel.2014.10.033.
Grover, J.P., 1990. Resource competition in a variable environment: phytoplankton growing according to monod's model. Am. Nat. 136, 771–789. https://doi.org/10.1086/285131.
Hansen, B., Bjørnsen, P.K., Hansen, P.J., 1994. The size ratio between planktonic predators and their prey. Limnol. Oceanogr. 39, 395–403. https://doi.org/10.4319/lo.1994.39.2.0395.
Hansen, P.J., Bjørnsen, P.K., Hansen, B., 1997. Zooplankton grazing and growth: scaling within the 2-2,000um body size range. Limnol. Oceanogr. 42, 687–704.
Hardin, G., 1960. The competitive exclusion principle. Science 131, 1292–1297. https://doi.org/10.1126/science.131.3409.1292.
Hillebrand, H., Acevedo-Trejos, E., Moorthi, S.D., Ryabov, A., Striebel, M., Thomas, P.K., Schneider, M., 2022. Cell size as driver and sentinel of phytoplankton community structure and functioning. Funct. Ecol. 36, 276–293. https://doi.org/10.1111/1365-2435.13986.
HilleRisLambers, J., Adler, P.B., Harpole, W.S., Levine, J.M., Mayfield, M.M., 2012. Rethinking community assembly through the lens of coexistence theory. Annu. Rev. Ecol. Evol. Syst. 43, 227–248. https://doi.org/10.1146/annurev-ecolsys-110411-160411.
Holt, R.D., 1977. Predation, apparent competition, and the structure of prey communities. Theor. Popul. Biol. 12, 197–229. https://doi.org/10.1016/0040-5809(77)90042-9.
Hutchinson, G.E., 1961. The paradox of the plankton. Am. Nat. 95, 137–145.
Irigoien, X., Flynn, K.J., Harris, R.P., 2005. Phytoplankton blooms: a 'loophole' in microzooplankton grazing impact? J. Plankton Res. 27, 313–321. https://doi.org/10.1093/plankt/fbi011.
Karakoç, C., Clark, A.T., Chatzinotas, A., 2020. Diversity and coexistence are influenced by time-dependent species interactions in a predator–prey system. Ecol. Lett. 23, 983–993. https://doi.org/10.1111/ele.13500.
Kneitel, J.M., Chase, J.M., 2004. Trade-offs in community ecology: linking spatial scales and species coexistence. Ecol. Lett. 7, 69–80. https://doi.org/10.1046/j.1461-0248.2003.00551.x.
Layden, A., Merchant, C., MacCallum, S., 2015. Global climatology of surface water temperatures of large lakes by remote sensing: global climatology of lake surface water temperatures. Int. J. Climatol. 35, 4464–4479. https://doi.org/10.1002/joc.4299.
Leibold, M.A., 1996. A graphical model of keystone predators in food webs: trophic regulation of abundance, incidence, and diversity patterns in communities. Am. Nat. 147, 784–812. https://doi.org/10.1086/285879.
Leibold, M.A., Norberg, J., 2004. Biodiversity in metacommunities: plankton as complex adaptive systems? Limnol. Oceanogr. 49, 1278–1289. https://doi.org/10.4319/lo.2004.49.4_part_2.1278.
Lewis, M., Smith, J., 1983. A small volume, short-incubation-time method for measurement of photosynthesis as a function of incident irradiance. Mar. Ecol. Prog. Ser. 13, 99–102. https://doi.org/10.3354/meps013099.
Limberger, R., Wickham, S.A., 2011. Predator dispersal determines the effect of connectivity on prey diversity. PLoS ONE 6, e29071. https://doi.org/10.1371/journal.pone.0029071.
Litchman, E., 1998. Population and community responses of phytoplankton to fluctuating light. Oecologia 117, 247–257. https://doi.org/10.1007/s004420050655.
Litchman, E., Klausmeier, C.A., Schofield, O.M., Falkowski, P.G., 2007. The role of functional traits and trade-offs in structuring phytoplankton communities: scaling from cellular to ecosystem level. Ecol Letters 10, 1170–1181. https://doi.org/10.1111/j.1461-0248.2007.01117.x.
Lubchenco, J., 1978. Plant species diversity in a marine intertidal community: importance of herbivore food preference and algal competitive abilities. Am. Nat. 112, 23–39. https://doi.org/10.1086/283250.
Lürling, M., 2021. Grazing resistance in phytoplankton. Hydrobiologia 848, 237–249. https://doi.org/10.1007/s10750-020-04370-3.
Marañón, E., Cermeño, P., López-Sandoval, D.C., Rodríguez-Ramos, T., Sobrino, C., Huete-Ortega, M., Blanco, J.M., Rodríguez, J., 2013. Unimodal size scaling of phytoplankton growth and the size dependence of nutrient uptake and use. Ecol. Lett. 16, 371–379. https://doi.org/10.1111/ele.12052.
McCauley, E., Briand, F., 1979. Zooplankton grazing and phytoplankton species richness: field tests of the predation hypothesis1: predation and algal diversity. Limnol. Oceanogr. 24, 243–252. https://doi.org/10.4319/lo.1979.24.2.0243.
Monod, J., 1949. The growth of bacterial cultures. Annu. Rev. Microbiol. 3, 371–394.
Oschlies, A., Schartau, M., 2005. Basin-scale performance of a locally optimized marine ecosystem model. J Mar Res 63, 335–358. https://doi.org/10.1357/0022240053693680.
Pomati, F., Shurin, J.B., Andersen, K.H., Tellenbach, C., Barton, A.D., 2020. Interacting temperature, nutrients and zooplankton grazing control phytoplankton size-abundance relationships in eight swiss lakes. Front. Microbiol. 10, 3155. https://doi.org/10.3389/fmicb.2019.03155.
Post, B., Acevedo-Trejos, E., Barton, A.D., Merico, A., 2024. The XSO framework (v0.1) and Phydra library (v0.1) for a flexible, reproducible, and integrated plankton community modeling environment in Python. Geosci. Model Dev. 17, 1175–1195. https://doi.org/10.5194/gmd-17-1175-2024.
Poulin, F.J., Franks, P.J.S., 2010. Size-structured planktonic ecosystems: constraints, controls and assembly instructions. J. Plankton Res. 32, 1121–1130. https://doi.org/10.1093/plankt/fbp145.
Prowe, A.E.F., Pahlow, M., Dutkiewicz, S., Follows, M., Oschlies, A., 2012. Top-down control of marine phytoplankton diversity in a global ecosystem model. Prog. Oceanogr. 101, 1–13. https://doi.org/10.1016/j.pocean.2011.11.016.
Roy, S., Chattopadhyay, J., 2007. The stability of ecosystems: a brief overview of the paradox of enrichment. J Biosci 32, 421–428. https://doi.org/10.1007/s12038-007-0040-1.
Ryabov, A.B., Morozov, A., Blasius, B., 2015. Imperfect prey selectivity of predators promotes biodiversity and irregularity in food webs. Ecol. Lett. 18, 1262–1269. https://doi.org/10.1111/ele.12521.
Saiz, E., Calbet, A., 2007. Scaling of feeding in marine calanoid copepods. Limnol. Oceanogr. 52, 668–675. https://doi.org/10.4319/lo.2007.52.2.0668.
Sarnelle, O., 2005. Daphnia as keystone predators: effects on phytoplankton diversity and grazing resistance. J. Plankton Res. 27, 1229–1238. https://doi.org/10.1093/plankt/fbi086.
Sommer, U., Sommer, F., 2006. Cladocerans versus copepods: the cause of contrasting top–down controls on freshwater and marine phytoplankton. Oecologia 147, 183–194. https://doi.org/10.1007/s00442-005-0320-0.
Steiner, C.F., 2003. Keystone predator effects and grazer control of planktonic primary production. Oikos 101, 569–577.
Steiner, C.F., 2001. The effects of prey heterogeneity and consumer identity on the limitation of trophic-level biomass. Ecology 82, 2495–2506. https://doi.org/10.1890/0012-9658(2001)082[2495:TEOPHA]2.0.CO;2.
Taherzadeh, N., Bengfort, M., Wirtz, K.W., 2019. A trait-based framework for explaining non-additive effects of multiple stressors on plankton communities. Front. Mar. Sci. 6, 351. https://doi.org/10.3389/fmars.2019.00351.
Taniguchi, D.A.A., Follows, M.J., Menden-Deuer, S., 2023. Planktonic prey size selection reveals an emergent keystone predator effect and niche partitioning. PLoS ONE 18, e0280884. https://doi.org/10.1371/journal.pone.0280884.
Tilman, D., 1982. Resource Competition and Community Structure. (MPB-17), 17. Princeton University Press. https://doi.org/10.2307/j.ctvx5wb72.
Vallina, S.M., Ward, B.A., Dutkiewicz, S., Follows, M.J., 2014. Maximal feeding with active prey-switching: a kill-the-winner functional response and its effect on global diversity and biogeography. Prog. Oceanogr. 120, 93–109. https://doi.org/10.1016/j.pocean.2013.08.001.
Ward, B.A., Dutkiewicz, S., Jahn, O., Follows, M.J., 2012. A size-structured food-web model for the global ocean. Limnol. Oceanogr. 57, 1877–1891. https://doi.org/10.4319/lo.2012.57.6.1877.
Weigel, B., Kotamäki, N., Malve, O., Vuorio, K., Ovaskainen, O., 2023. Macrosystem community change in lake phytoplankton and its implications for diversity and function. Glob. Ecol. Biogeogr. 32, 295–309. https://doi.org/10.1111/geb.13626.